Proceedings World Geothermal Congress 2015
Melbourne, Australia, 19-25 April 2015

Developing the 'Heat Needle'—a Tool for Cost Effective Heat Flow Mapping

Graeme R. Beardsmore and Anson Antriasian

Hot Dry Rocks Pty Ltd, PO Box 251, South Yarra, Victoria 3141, AUSTRALIA

graeme.beardsmore@hotdryrocks.com

Keywords: Heat flow, geophysics, mapping, exploration, temperature gradient, thermal conductivity

ABSTRACT

Conductive heat flow is arguably the only measurable surface expression of the thermal state of the crust at any given location. The Heat Needle is a tool designed to detect variations in geothermal heat flow from measurements made within the top meter of the earth. At these shallow levels, the geothermal component of heat flow (average ~0.06 W/m^2) is dominated by solar irradiation (average daily peak ~300 W/m^2). To overcome this, the Heat Needle is designed to record time-series temperature data at the surface and at 20 cm intervals from 10 cm to 110 cm subsurface, and to use frequency-domain filtering to increase the geothermal-to-solar signal ratio. Vertical thermal conductivity is derived from a combination of vertical thermal diffusivity measurements and radial heat injection tests. The goal is to develop the Heat Needle as a cost effective geophysical tool for mapping the extent and magnitude of thermal anomalies prior to test drilling. The target is to detect surface heat flow variations on the order of 0.01 W/m^2. This requires several orders of magnitude greater sensitivity than existing shallow temperature and heat flow mapping methods. The technical challenges of the Heat Needle revolve around achieving the necessary precision, accuracy, durability, reliability, thermal bulk, cost, usability and power efficiency for the probe; as well as designing appropriate field procedures, data processing algorithms and interpretation strategies. As of September 2014, a laboratory process had been refined to calibrate temperature sensors to an absolute accuracy of ±0.0024°C (1 σ). Radial heat injection tests had been performed and analyzed. Eight Heat Needles had been deployed and successfully recovered during a field trial of approximately nine-months duration in a remote part of South Australia. That survey generated close to one million, high precision (±0.0003°C), high accuracy (±0.0024°C) temperature records as a robust data set for developing and testing algorithms for data reduction and interpretation. A subsequent twelve-month trial over four geothermal sites had commenced in Mexico.

1. INTRODUCTION

1.1. Background

For the past few years, Hot Dry Rocks Pty Ltd (HDR: Australia) has been developing and testing a tool and methodology to reliably, accurately and precisely measure conductive heat flow in the top meter of the earth's crust. HDR has dubbed the tool the 'Heat Needle'. The driving motivation behind the Heat Needle is to remove a critical barrier to regional heat flow mapping—namely the requirement for fully cored boreholes to depths greater than 100 m. HDR's ultimate objective is to develop the Heat Needle into a new geophysical survey system to generate 'heat anomaly' maps. Such maps would delineate the extent and magnitude of anomalous sub-surface heat sources in the same way that existing geophysical techniques currently delineate anomalous subsurface density (gravity technique), magnetic susceptibility (magnetics technique), electrical properties (MT, TEM etc techniques; Figure 1), sonic velocity (seismic tomography) and other geophysical properties.

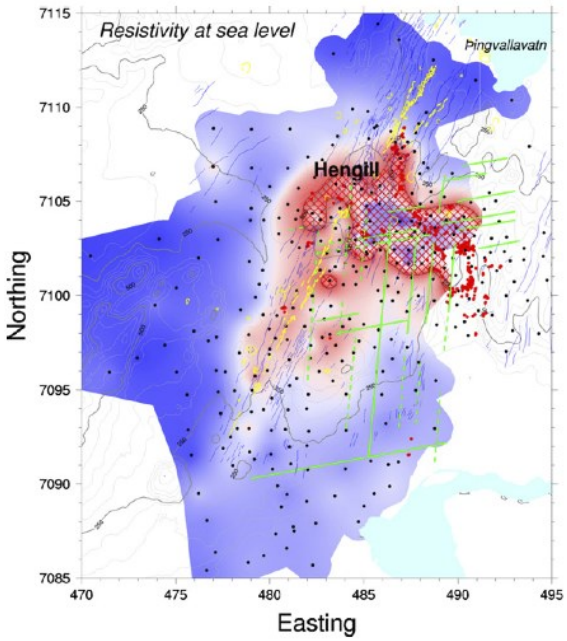

Figure 1: A resistivity depth slice map from Árnason *et al.* (2010) as an illustration of how a heat anomaly map might eventually be presented.

Heat anomaly maps would provide an additional layer of geophysical data valuable for exploration for geothermal energy, accumulations of radioactive minerals, ground water flow paths, salt diapirs and other phenomena that influence the magnitude and direction of heat flow in the crust. At present, heat flow mapping at a prospect scale is prohibitively expensive due to the requirement for boreholes that penetrate beneath the thermal influence of the seasonal surface temperature cycle (about 30 m; Beardsmore and Cull, 2001). The Heat Needle, however, is placed into the top meter of soil, so could be deployed over wide areas at just a fraction of the cost of obtaining a single heat flow measurement using a deep borehole.

The main challenge to measuring the geothermal component of conductive heat flow close to the Earth's surface is the thermal disturbance of the diurnal and seasonal temperature cycles. At any given moment and location, the periodic ebb and flow of solar energy in the top meter of the earth (up to 300 W/m^2) can be 5,000 times that of the constant geothermal heat flow from the Earth (about 0.06 W/m^2). HDR has designed the Heat Needle with a sensitivity to detect the small geothermal signal from within the solar 'noise'. The strategy is to collect a precise and accurate time-series of shallow heat flow measurements, which are then processed to remove the 'high frequency' daily transients. Beardsmore (2012) reported on HDR's progress up until the start of 2012. This paper presents more details about the critical components of the Heat Needle, and the outcomes of developments and field trials as of September 2014.

1.2. Conceptual basis of the Heat Needle

Vertical conductive heat flow is the product of vertical thermal gradient and vertical thermal conductivity. In many places, vertical thermal conductivity remains relatively constant through time (the Heat Needle will likely fail to delineate geothermal heat flow in places where this assumption does not hold true, such as soils that experience significant variations in water content through time) but the vertical thermal gradient at shallow depths is almost always grossly disturbed by the daily and annual solar cycles. The Heat Needle is designed to record a time-series of precise temperatures at regular time and depth intervals. During a survey, several Heat Needles are deployed along a survey line or in a grid to simultaneously collect data over a period of weeks to months.

Where the assumption of pure conduction holds in the top meter of the Earth, changes in temperature at the Earth's surface diffuse into the ground in a manner that can be characterized by (Carslaw and Jaeger, 1959, p58):

$$T_\theta = \Delta T \text{ x } \mathrm{erfc}[z/(2\sqrt{(\kappa t)})] \quad (1)$$

where T_θ is the departure from the original equilibrium temperature at time, t, and depth, z, due to a step change in surface temperature of ΔT at time $t = 0$; κ is the thermal diffusivity; 'erfc()' is the 'complimentary error function.' The temperature at any depth, z, is the natural equilibrium temperature plus the sum of the effects of all historical changes in surface temperature.

Changes in surface temperature are dominated by two periodic cycles; the 24-hour diurnal cycle and the 365-day annual cycle. Simplistically, the time varying temperature gradient in the top meter of the ground, $G_o(t)$, is the sum of three individual components:

$$G_o(t) = G_g + G_d(t) + G_a(t) \quad (2)$$

where G_g is the equilibrium geothermal gradient, $G_d(t)$ is the variable gradient due to the diurnal cycle, and $G_a(t)$ is the variable gradient due to the annual cycle. Precise time-series records over several months should allow us to effectively filter $G_d(t)$ from the record though the application of an appropriate low pass filter. If we assume that the annual surface temperature signal is broadly constant across a survey area, then lateral variations in observed gradient during a survey are due to variations in the underlying geothermal gradient and thermal diffusivity of the ground. This should ultimately allow us to map lateral variations in relative (rather than absolute) heat flow to reveal local thermal anomalies.

1.3. Previous shallow thermal probes

Heat flow probes of various forms have been routinely used to determine heat flow in the deep ocean since the 1950's. The first probes were essentially strings of thermistors with no *in situ* thermal conductivity measuring capabilities (Bullard, 1954; Gerard *et al.*, 1962). These evolved in the late 1960's and early 1970's to include an *in situ* thermal conductivity sensor in the form of a line-source heater (Hyndman *et al.*, 1978). For example, Christoffel and Calhaem (1969) described a heat flow probe for use in soft sediments. The six-foot long, cylindrical, steel probe incorporated four thermistors and a line-source thermal conductivity sensor in the form of a coil of heating wire wrapped around the probe. They reported testing the probe in relatively shallow water in Wellington Harbor (New Zealand), but did not report any experiments on land.

Shallow temperature surveys are sometimes used to delineate relatively high temperature, convecting geothermal systems. These are associated with high shallow temperature gradients, which make anomalies relatively easy to detect. Most of these surveys require inserting thermistor probes 1–2 m into the ground, and allowing the temperatures to equilibrate. Some authors have devised methods of correcting for near-surface effects such as the annual solar cycle (e.g. Olmsted and Ingebritsen, 1986).

Coolbaugh *et al.* (2007) described a methodology to detect 'blind' geothermal systems (i.e. those systems that do not have surface features such as hot springs and geysers) using ground temperature measurements at a depth of two meters. They constructed 2.2 m long, hollow, thin, cylindrical steel probes within which they placed several platinum resistance (RTD) thermometers. A hammer-drill, run by a generator, was used to drive the probes into the ground. One or more base stations were set up to monitor the drift in ground temperature due to seasonal effects during a survey, which could last several days. The base station drift was used to correct the temperatures recorded across all the survey stations, although their correction did not account for variations in the thermal diffusivity of the soil. The same group later reported corrections for thermal diffusivity, for variations in surface albedo (Coolbaugh *et al.*, 2010), and for transient weather events (Sladek *et al.*, 2012). The method detected thermal anomalies on the order of ±0.5°C at two meters depth.

Hurwitz *et al.* (2012) demonstrated the principle of conductive heat flow mapping with surveys over two areas within the Yellowstone Plateau Volcanic Field in the United States. Their results clearly delineated the extent of surface heat flow anomalies associated with thermal features at the surface, to a precision of about ±10 W/m^2 (Figure 2). HDR has designed the Heat Needle to generate similar maps but at three orders of magnitude greater precision.

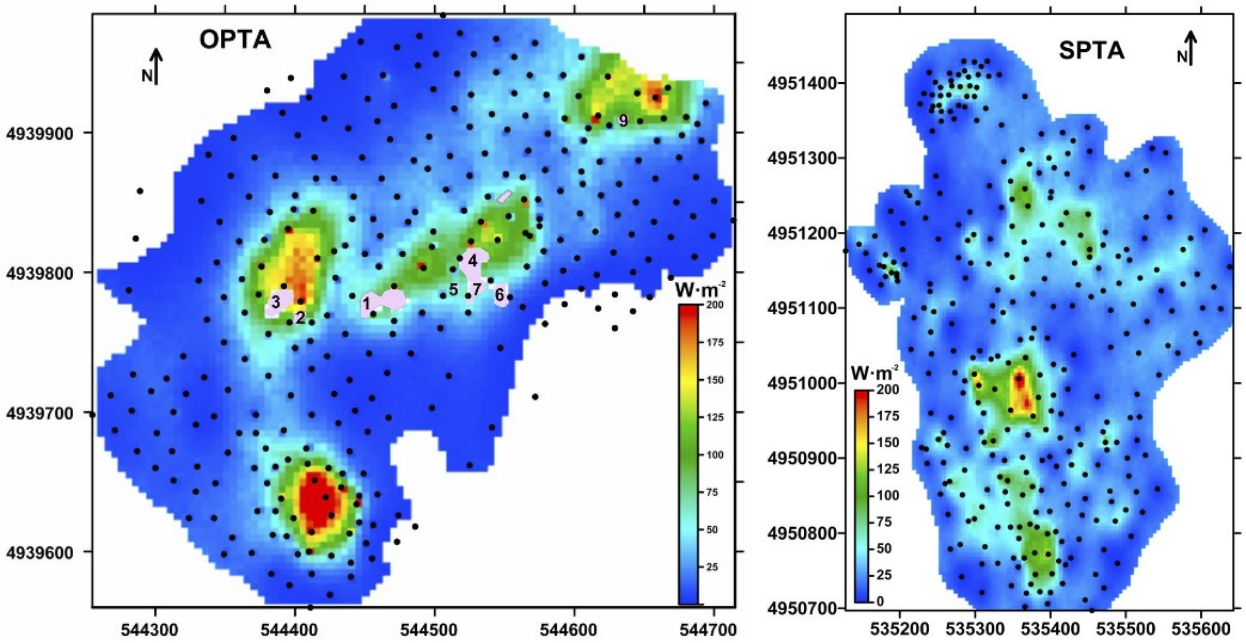

Figure 2: Surface heat flow maps around the Obsidian Pool Thermal Area (left) and Solfatara Plateau Thermal Area (right) within the Yellowstone National Park, USA, bounded by a temperature gradient of 1 °C/m. Black dots are locations of temperature–depth measurements; pink patches with numbers show the locations of surface hot pools. From Hurwitz *et al.* (2012).

1.4 Design criteria for the Heat Needle

The Heat Needle is intended as a prospecting tool for commodities beyond hydrothermal geothermal systems. Specifically, it is designed to be prospecting tool for uranium bearing 'iron oxide, copper, gold' ore bodies (IOCG-U's) in central Australia. Modeling and previous observations (e.g. Houseman *et al.*, 1989) suggest that economically important IOCG-U deposits create local heat flow anomalies on the order of 10's of milli-watts per square meter, due to the radioactive decay of the uranium. To be a useful prospecting tool in central Australia, therefore, the Heat Needle must meet a meticulous set of design criteria:

- Strong enough to withstand repeated insertion and removal from the ground;
- Temperature sensors accurate to at least ±5 mK and precise to at least ±1 mK;
- Operating temperature range 0–50°C;
- Minimal drift in sensor and electronics response with time and temperature;
- Vertical thermal conductivity measured *in situ* to better than ±5% accuracy;
- Low thermal bulk for rapid thermal equilibration;
- Thermal conductance similar to ground so as to not disturb natural thermal state;
- Sensor depth accurate to ±10 mm;
- Data stored directly to memory;
- Environment and abrasion resistant;
- Power source and memory for up to 12 months of continuous data collection;
- Data collection once every 15 minutes;
- Reliable, repeatable, portable, safe tool insertion and removal;
- Cheap enough for mass production.

Of these, the greatest challenges have been to develop the sensors necessary to measure the physical properties of temperature gradient and vertical thermal conductivity to the required precision and accuracy. The following sections describe HDR's solutions to these challenges.

2. TEMPERATURE SENSORS

2.1 Design constraints

The purpose of the Heat Needle is to detect and map variations in conductive heat flow on the order of ±0.010 W/m^2. In most regolith materials, this calls for resolution of thermal gradient to about ±0.005 °C/m. Designing a tool to accurately measure such precise thermal gradients over a temperature range of 50°C and a depth interval of one-meter is a significant challenge. The temperature sensors within the tool must reliably and accurately determine temperature at sub-milli-kelvin precision and milli-kelvin accuracy over a 50 K range. The temperature sensors are, therefore, the critical components of the Heat Needle. Seven

temperature sensors are incorporated into each assembled Heat Needle. When the Heat Needle is correctly deployed, the sensors sit at ground surface level, and at 10 cm, 30 cm, 50 cm, 70 cm, 90 cm and 110 cm depth below ground surface.

Thermistors provide the only practical sensor to achieve the necessary sensitivity over the required temperature range. Thermistors are electronic components whose electrical resistance is a strong function of temperature. A precise measurement of the electrical resistance across a thermistor is sufficient to calculate the temperature of the thermistor to milli-kelvin precision. However, no two thermistors have exactly the same response to temperature, so the *absolute accuracy* of the temperature measurement depends entirely on the accuracy with which the thermistors are calibrated and subsequently interrogated.

The electrical resistance of typical thermistors varies on the order of 10's of ohms per kelvin. Milli-kelvin precision therefore requires precise and accurate measurements of electrical resistance on the order of 10's of milli-ohms. Two issues arise when such accuracy and precision are required. Both issues relate to the fact that, in practice, a measurement of electrical resistance requires a measurement of voltage drop due to a known current passing through the thermistor.

The first issue is *self-heating* of the thermistor. Any resistor dissipates electrical power in the form of heat following the relationship $P = I^2 \cdot R$, where P is the dissipated power in watts, I is the current in amps, and R is the resistance in ohms. This power dissipation manifests itself as a self-heating of the thermistor according to $\mathrm{d}T/\mathrm{d}t = P / m \cdot c_\mathrm{p}$ (where $\mathrm{d}T/\mathrm{d}t$ is the self-heating rate in K/s, m is the mass of the thermistor in kg, and c_p is the specific heat capacity of the thermistor in J/kgK) $= I^2 \cdot R / m \cdot c_\mathrm{p}$. Typical properties for a small thermistor are R = 1,000 Ω, c_p = 850 J/kgK and $m = 6 \cdot 10^{-6}$ kg, which implies a self-heating rate of $2 \cdot 10^5 \cdot I^2$ K/s. Just one milli-amp provides sufficient power to heat a typical thermistor at a rate of 200 mK/s! Given that a practical measurement of resistance might take up to half a second, it follows that a temperature measurement to milli-kelvin precision can only be obtained if current is limited to much less than 1 mA. And, because $V = I \cdot R$, the resultant voltage measured across the thermistor is much less than 1 V across the full measurement range of the Heat Needle. Milli-kelvin precision over a 50 K dynamic range therefore requires an accurate micro-voltmeter with >>50,000 steps.

The second issue is to ensure that variations in resistance measured by the voltmeter are entirely due to changes in the temperature of the sensor. A voltmeter measures the difference in electrical potential across its two input terminals. These terminals are necessarily connected to the thermistor via lengths of wire. The connecting wires and junctions themselves contribute to the electrical resistance observed by the voltmeter. If the wires or junctions are subject to changes in temperature during a survey (due to environmental conditions) then these will also affect the measured resistance.

The above two issues, as well as others related to the limited space in which the sensors must operate within the Heat Needle, imposed severe constraints on the design of the temperature sensor components. The solution was to house all electronic components of the temperature sensor system on integrated circuit boards (Figure 3), linked via ribbon cables internally within the Heat Needle and to an external power source and digital logging system at the surface. Each circuit board incorporates a Wheatstone bridge circuit, voltmeter, amplifier, analog–digital converter, a controller chip and sundry other electronic components. In short, each board holds all the circuitry required to generate a precise digital representation of the electrical resistance of the on-board thermistors and to transmit this digital value to the surface. The output of the circuit is a 17-bit digital value between -65,536 and +65,535 directly related to temperature, with the zero point at approximately 25°C and an average sensitivity of about 0.4 mK per digital bit. Importantly, the entire board is exposed to approximately the same temperature at any given moment, so all temperature-dependent characteristics of the board can be simultaneously characterized through a calibration process.

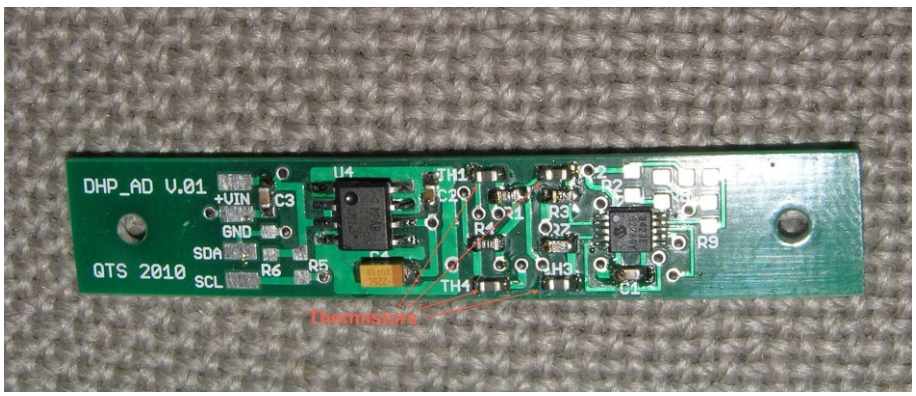

Figure 3: A temperature sensor board for the Heat Needle, showing four on-board thermistors. The circuit board is approximately 10 mm wide by 60 mm long. Other on-board components include a voltmeter, amplifier, analog–digital converter and controller chip. Power and signal communications are provided via the four solder pads at the left end.

The seven sensor boards in each Heat Needle are joined in series with ribbon cables, and each sensor board has its own unique digital identity. Power is provided to the string of sensor boards by a battery pack housed within a control box at the surface. The control box is programmed to open communications with the sensor string at regular intervals, and to receive and store the digital signals from the six sensor boards. The Heat Needle hibernates between readings to conserve energy and maximize battery life.

2.2 Calibration

Precision calibration of the temperature sensor boards is central to the operation of the Heat Needle. The thermistors are the key temperature sensitive components on the sensor boards. The relationship between temperature and electrical resistance for any given thermistor can be described using the Steinhart-Hart equation (Steinhart and Hart, 1968):

$$\frac{1}{T} = A + B \cdot \ln(R) + C\left(\ln(R)\right)^3 \quad (3)$$

where T = temperature in kelvin; R = resistance in ohms; A, B, C = Steinhart-Hart coefficients. Each thermistor has a unique set of Steinhart-Hart coefficients, which means that each sensor board intrinsically has a unique temperature response curve and maximum accuracy is only achieved if each board is individually calibrated. However, the performances of other components on the boards (e.g. amplifier, standard resistors, analog-to-digital converter etc) also vary over the temperature range in which the Heat Needles are designed to operate. While their responses are far less sensitive to temperature than the thermistors' responses, they nonetheless exert enough impact on the overall response curves of the sensor boards that they invalidate the Steinhart-Hart equation as a basis for calibration. An empirical calibration process was, therefore, developed and employed as follows.

A Fluke 1529 digital thermometer calibrated by the National Measurement Institute (NMI) of Australia provides HDR's 'absolute' reference temperature. NMI quotes the absolute accuracy of the calibrated thermometer at ±0.002 K (1 σ) over the 0–50°C range. A set of Heat Needle sensor boards is simultaneously calibrated by suspension in close proximity to the sensor of the reference thermometer within a controlled temperature bath filled with mineral oil. The temperature of the bath is gradually increased in approximately 5 K increments from about 0°C to about 55°C, held steady at each of the 12 temperature levels for at least 20 minutes (Figure 4). The reference thermometer records the bath temperature to 0.1 mK precision at 2 s intervals, while the digital responses of the sensor boards are simultaneously recorded at one-bit (~0.3 mK) precision every 30 s.

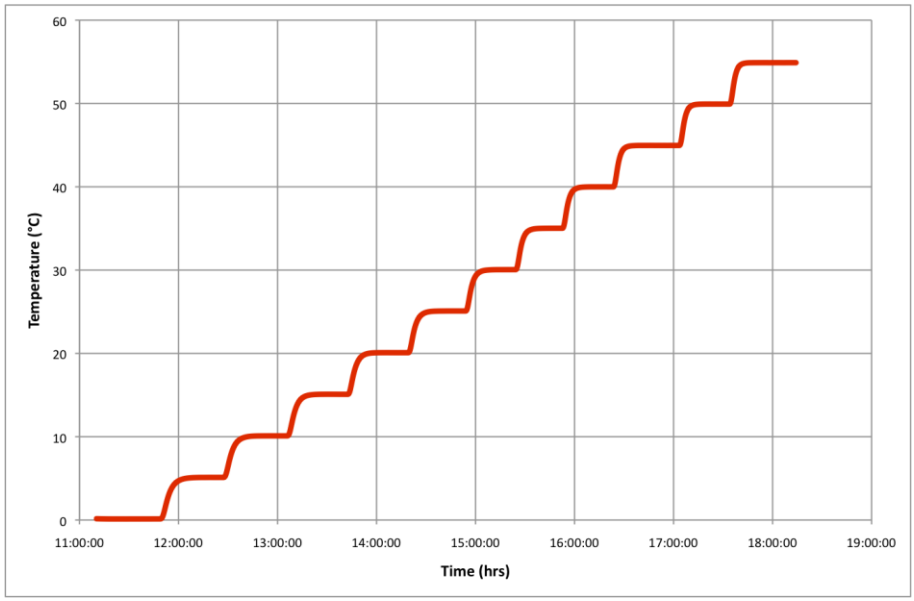

Figure 4: A typical temperature–time pathway for a calibration run provides 12 precision temperature calibration points.

The data for each of the 12 quasi-stable temperature steps are subsequently assessed to identify 12 intervals of several minutes' duration within which the reference temperature and board responses are all stable within ranges of about 1 mK and 3 bits, respectively. The average temperature and board responses for each of these time intervals are noted (e.g. Table 1). At the end of this process, 12 precise temperature-versus-board-response calibration points are defined for each of the sensor boards over the temperature range 0–55°C (e.g. Table 2, Figure 5).

HDR has found from experience that a seventh order polynomial function fits the 12 temperature-versus-board-response calibration points to within a fraction of a milli-kelvin in virtually every case. This is an empirical observation with no obvious physical explanation, but it allows the temperature sensitivity of each sensor board to be characterized by eight calibration coefficients. Given that each Heat Needle holds six subsurface sensor boards, a full calibration of a Heat Needle generates a matrix of 48 coefficients, each defined to six significant digits (e.g. Table 3). The temperature (°C) of the i^{th} sensor board at any given time can be calculated by substituting the digital output of the sensor board (S_i) at that time into Equation 4:

$$T = A_i S_i^7 + B_i S_i^6 + C_i S_i^5 + D_i S_i^4 + E_i S_i^3 + F_i S_i^2 + G_i S_i + H_i \quad (4)$$

Where A_i through to H_i are the calibration coefficients of the i^{th} sensor board.

As of September 2014, HDR does not carry out a precise calibration for the 'surface' temperature sensor. The purpose of that sensor is for correlation of surface temperature patterns between Heat Needles, so high temperature precision is not required.

Table 1: Examples of stable two-minute intervals of reference temperature and sensor board responses during calibration

Time	Temperature	Board 1	Board 2	Board 3	Board 4	Board 5	Board 6
11:39:15	0.1303 °C	-78997	-79885	-78741	-79611	-78510	-79730
11:39:45	0.1302 °C	-78999	-79886	-78741	-79612	-78510	-79730
11:40:15	0.1301 °C	-78997	-79886	-78742	-79612	-78509	-79730
11:40:45	0.1301 °C	-78998	-79886	-78742	-79613	-78510	-79731
11:41:15	0.1302 °C	-78998	-79887	-78742	-79612	-78509	-79730
Average	**0.13018 °C**	**-78997.8**	**-79886.0**	**-78741.6**	**-79612.0**	**-78509.6**	**-79730.2**
…	…	…	…	…	…	…	…
15:22:15	30.0548 °C	17699	16384	17887	16786	18289	16668
15:22:45	30.0554 °C	17700	16386	17888	16788	18291	16670
15:23:15	30.0555 °C	17701	16387	17888	16789	18291	16671
15:23:45	30.0556 °C	17701	16386	17888	16788	18291	16669
15:24:15	30.0550 °C	17701	16386	17887	16787	18291	16670
Average	**30.05526 °C**	**17700.4**	**16385.8**	**17887.6**	**16787.6**	**18290.6**	**16669.6**
…	…	…	…	…	…	…	…

Table 2: Examples of precise temperature-versus-board-response calibration points for a set of six Heat Needle boards

Temperature (°C)	0.13018	5.11444	10.10148	15.09662	20.08710	25.09096	30.05526	35.02204	39.99102	44.95940	49.92830	54.89774
Board 1	-78997.8	-64023.2	-48103.6	-31568.6	-14842.8	1750.8	17700.4	32871.0	47053.8	60107.4	71969.6	82634.0
Board 2	-79886.0	-65038.0	-49229.2	-32783.4	-16119.6	441.0	16385.8	31575.2	45794.6	58900.6	70825.4	81560.4
Board 3	-78741.6	-63773.4	-47862.0	-31337.2	-14626.4	1954.0	17887.6	33040.8	47205.4	60241.4	72088.0	82736.8
Board 4	-79612.0	-64728.6	-48887.6	-32416.2	-15734.4	838.8	16787.6	31973.6	46187.4	59282.0	71193.0	81909.8
Board 5	-78509.6	-63490.0	-47536.0	-30978.2	-14242.2	2353.2	18290.6	33437.8	47588.4	60604.2	72424.6	83046.4
Board 6	-79730.2	-64855.8	-49021.4	-32550.4	-15866.4	713.0	16669.6	31866.4	46093.0	59201.8	71127.0	81858.6

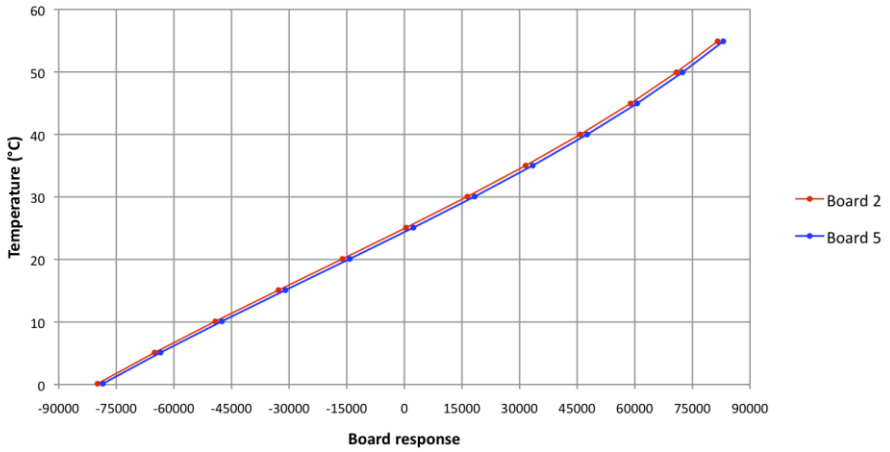

Figure 5: A graph of the calibration points for Board 2 (red) and Board 5 (blue) from Table 2.

Table 3: Example of a full calibration matrix for a Heat Needle. For any given output (S_i) of sensor board 'i', temperature can be calculated using Equation 4.

	A (x 10^{-36})	B (x 10^{-31})	C (x 10^{-26})	D (x 10^{-21})	E (x 10^{-15})	F (x 10^{-10})	G (x 10^{-4})	H
Board 1	4.65247	3.86984	9.60263	6.55248	4.21502	2.77072	3.04344	24.5571
Board 2	4.63227	3.70836	9.64900	6.82307	4.25023	2.78547	3.05445	24.9560
Board 3	5.18929	3.73800	9.00853	6.61168	4.24391	2.75962	3.04502	24.4948
Board 4	4.97038	3.78961	9.27625	6.68260	4.24616	2.77340	3.05072	24.8348
Board 5	5.03357	3.86320	9.05402	6.59326	4.24120	2.76438	3.04085	24.3738
Board 6	4.66764	3.86307	9.59764	6.53599	4.23145	2.77199	3.05019	24.8734

The final step in the calibration process is to repeat the entire calibration two or three times to demonstrate consistency of outcomes. An acceptable calibration of a Heat Needle is one that produces a coefficient matrix that generates temperature values varying by no greater than 2 mK relative to an independent calibration for all six sensor boards over the temperature range 0–50°C. This equates to a calibration uncertainty no greater than ±1.2 mK (1 σ), and an absolute measurement uncertainty no greater than ±2.4 mK (1 σ) for each Heat Needle sensor board when the absolute accuracy of the reference thermometer is also taken into account. The result is a fully calibrated Heat Needle that can resolve temperature gradient to a precision of about ±0.0005 °C/m with an absolute accuracy of about ±0.0024 °C/m (1 σ) over a depth interval of one meter.

3. THERMAL PROPERTY MEASUREMENTS

3.1 Theory

The Heat Needle is designed to measure vertical conductive heat flow in the top meter of the ground. This requires measurements of both the vertical thermal gradient (discussed in the sections above) and vertical thermal conductivity. There are two possible strategies to measure the vertical thermal conductivity in the vicinity of the Heat Needle when embedded in the ground. The first is to measure the horizontal (radial) thermal conductivity at a number of positions along the Heat Needle, and then to calculate the vertical conductivity as the harmonic mean of the measured horizontal conductivities. The number of points that can be measured is limited to the number of temperature sensors in the Heat Needle, and the measurements are most sensitive to the properties of the soil directly level with the sensors.

The second strategy is to multiply the vertical thermal diffusivity (which can be precisely derived from the diffusion of the daily heat cycle into the ground) by the volumetric heat capacity of the ground. Volumetric heat capacity is the product of density and specific heat capacity, but can also be calculated as thermal conductivity divided by thermal diffusivity. It is a scalar quantity so a measurement of volumetric heat capacity derived from a radial heat pulse can be multiplied directly by the vertical thermal diffusivity to derive the vertical thermal conductivity.

Both strategies described above require an active heat pulse from the Heat Needle into the ground, so the Heat Needle includes an active heating circuit that runs from approximately ground level to just below the deepest sensor to inject a constant rate of heat into the surrounding soil. In this way, it is designed to operate as a large transient heat pulse ‘needle probe’ like those available at much smaller scale from many commercial suppliers. A needle probe can be approximated mathematically as an infinite cylindrical source of heat if its length-to-diameter ratio is greater than 25:1 (Jeffry *et al*., 1979). The diameter of the Heat Needle is 16 mm, so it approximates an infinite cylinder at points along its length that are 200 mm (20 cm) or greater from either of its ends. This condition is satisfied at the positions of the four temperature sensors between 30 cm and 90 cm depth. At those depths, heat conduction theory predicts that the rate of temperature increase recorded by the sensors in response to a constant rate of heating will approach a relationship appropriate for an infinite line source of heat:

$$\frac{\Delta T}{\ln(t)} = \frac{Q}{4\pi\lambda} \tag{5}$$

where ΔT is the change in temperature (K) since heating commenced, $\ln(t)$ is the natural logarithm of the time (seconds) since heating commenced, Q is the heating rate (W/m), and λ is the horizontal (radial from the Heat Needle) thermal conductivity of the ground (W/mK). For a known heating rate Q, it is relatively trivial to calculate λ once ΔT versus $\ln(t)$ reaches linearity.

In order to derive the volumetric heat capacity of the ground, however, the Heat Needle must measure both the thermal conductivity and thermal diffusivity of the surrounding soil. Kömle *et al*. (2011) published a full solution for the temperature of the soil near an embedded infinite cylindrical heat source:

$$T(r,t) = T_\infty + \frac{Q}{4\pi\lambda}\int_{t'=0}^{t}\frac{1}{(t-t')}\exp\left(-\frac{r^2+a^2}{4\kappa(t-t')}\right)dt' + \frac{Q}{4\pi\lambda}\int_{t'=0}^{t}\frac{1}{(t-t')}\exp\left(-\frac{r^2+a^2}{4\kappa(t-t')}\right)\left[I_0\left(\frac{ra}{2\kappa(t-t')}\right)-1\right]dt' \tag{6}$$

where r is radial distance (m) from the axis of the cylinder, a is the radius (m) of the cylinder, t is time (s) since heating commenced, T_∞ is the undisturbed temperature (°C) of the ground, Q is the heating rate (W/m), λ is the horizontal thermal conductivity (W/mK) of the soil, κ is the horizontal thermal diffusivity (m^2/s) of the soil, and I_0 denotes the modified Bessel function of the first kind and zeroth order. If we are only interested in the temperature at the face of the cylinder, then $r = a$ and Equation 6 reduces to:

$$T(t) = T_\infty + \frac{Q}{4\pi\lambda}\int_{t'=0}^{t}\exp\left(\frac{-a^2}{2\kappa(t-t')}\right)dt' + \frac{Q}{4\pi\lambda}\int_{t'=0}^{t}\frac{1}{(t-t')}\exp\left(\frac{-a^2}{2\kappa(t-t')}\right)\left[I_0\left(\frac{a^2}{2\kappa(t-t')}\right)-1\right]dt' \tag{7}$$

For the Heat Needle, the heating rate Q is fixed at 16.6 W/m (±1%) and the radius a is fixed at 0.008 m. A record of $T(t)$ during a heating experiment provides a curve that (theoretically) is a function only of variables λ and κ. A best fit of Equation 7 to the data should, in principle, reveal unique values for λ and κ.

3.2 Example data

Figure 6 shows an example of data generated during a real application of the Heat Needle to measure the thermal properties of the ground. The graphs show the time–temperature curves recorded at the six subsurface sensor depths due to a constant heating rate of 16.6 W/m (± 1% uncertainty) generated by the Heat Needle over a 50-minute period. The logarithmic time scale allows the display of temperatures recorded at the indicated depths at 2 s intervals over the first two minutes, and at 30 s intervals for the remaining time.

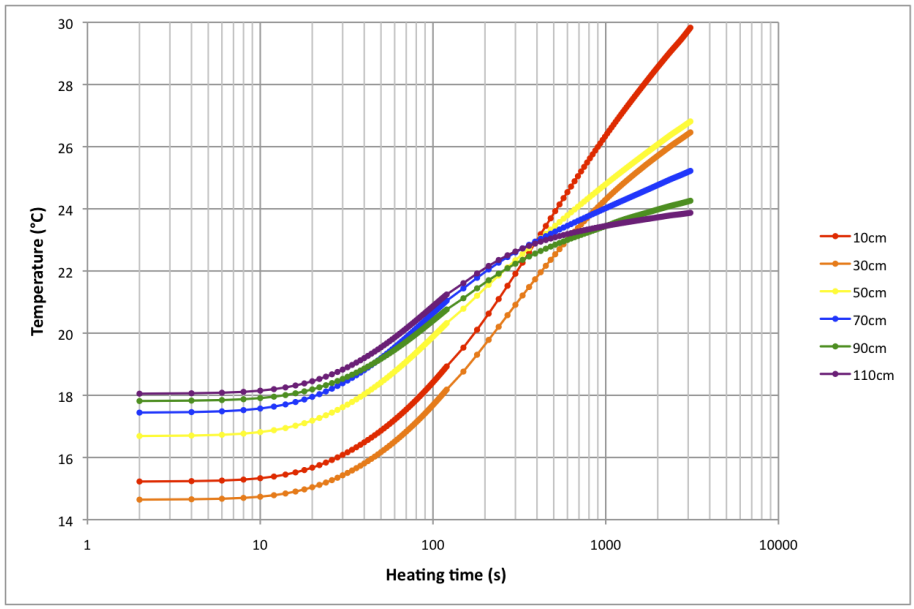

Figure 6: Temperature recorded by the six subsurface temperature sensors in a Heat Needle over a 50-minute heating period.

Figure 7 highlights the last 10 minutes of data for the sensors between 30 cm and 90 cm shown on Figure 6, illustrating that the temperature increase is close to linear with respect to the log of time. Assuming that the Heat Needle approximates an infinite line source of heat, the gradient of each line on Figure 7 is inversely proportional to the thermal conductivity of the surrounding medium at that depth (Equation 5). Given that the heating rate was 16.6 W/m, and carrying through the uncertainties in heating rate and recorded temperatures, the gradients of the lines on Figure 7 imply thermal conductivities of 0.791 ± 0.009 W/mK, 0.799 ± 0.009 W/mK, 1.279 ± 0.016 W/mK and 2.101 ± 0.029 W/mK at 30 cm, 50 cm, 70 cm and 90 cm depth, respectively. While these values were not independently verified by other means, they are consistent with the observed soil layering at the test site. The harmonic mean of these four horizontal thermal conductivity values gives an estimate of the bulk *vertical* thermal conductivity between about 20 cm and 100 cm depth: 1.060 ± 0.013 W/mK. The uncertainty is about ±1.25% (1 σ). This is well within the target accuracy of ±5%, but does not incorporate uncertainties due to limited depth sampling.

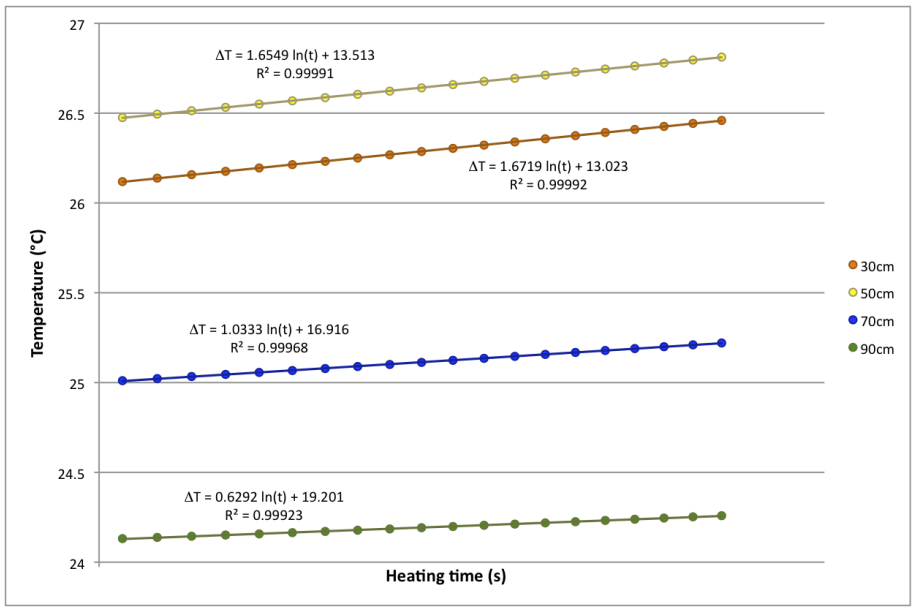

Figure 7: Last 10 minutes of data for four sensors of the recording shown on Figure 6.

4. FIELD TRIALS

4.1 Carrapateena IOCG-U ore body, South Australia

HDR deployed Heat Needles along a transect across a known IOCG-U ore body on the Stuart Shelf near the Carrapateena Arm of Lake Torrens in South Australia from early December 2012 to late August 2013 (Figure 8; Figure 9). The deployment was designed to test the ability of the Heat Needle to detect the thermal signature of the ore body. The surface geometry and composition of the ore body are well known from a comprehensive drilling program carried out by Oz Minerals Ltd, the owner and developer of the ore body. The deployment was also to test the durability of the Heat Needle hardware and software, and the deployment strategy. The survey provided a wealth of real field data and valuable experience that guided the development of the subsequent model of Heat Needle.

Figure 8: Lawrence Molloy prepares to deploy a Heat Needle at Carrapateena, South Australia.

Figure 9: A Heat Needle (foreground) deployed in South Australia. The one meter long power and communications cable runs from the underground sensor string to the control box housed within beneath the sunshade.

The physical deployment of the Heat Needles was challenging in the geological setting of the Stuart Shelf. An intention to pre-drill the holes for the Heat Needles using an extended length, premium quality masonry bit could not be achieved after a weld on the bit broke on the first drilling attempt. Each Heat Needle was tipped with its own masonry bit (Figure 8) but a very hard layer of silcrete 50–70 cm beneath the surface proved impossible to penetrate using the hand operated electric drill in several locations. Heat Needles could only be embedded to their full length (1,600 mm including drill bit) at eight of 12 locations attempted. The batteries

on the logger units of two of those eight failed after just a few days. The remaining six Heat Needles, however, operated as planned. They generated almost nine months of temperature data (Figure 10; Figure 11) and corresponding thermal property data.

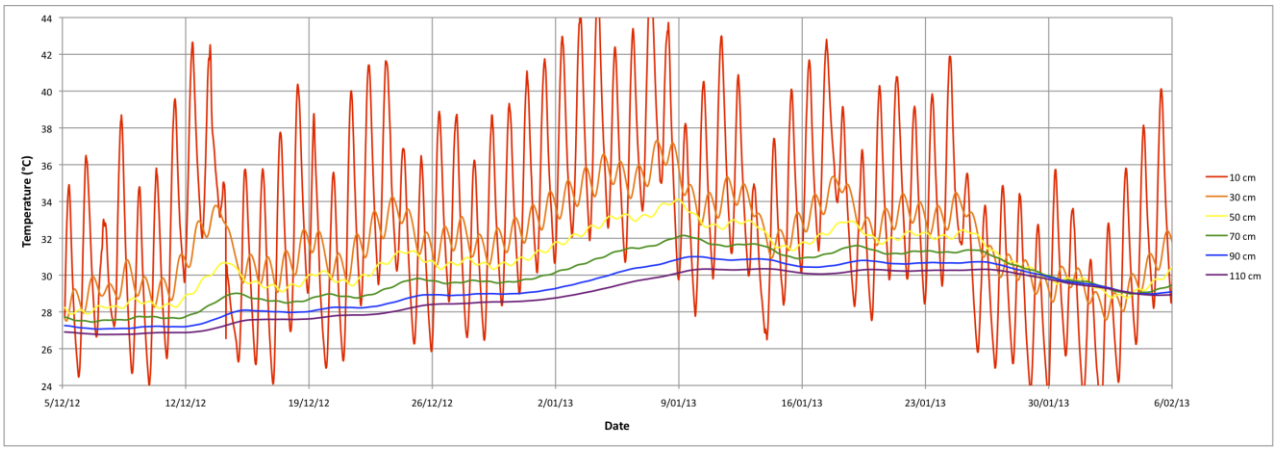

Figure 10: The first two months of subsurface temperature data recorded by one of the Heat Needles installed at Carrapateena.

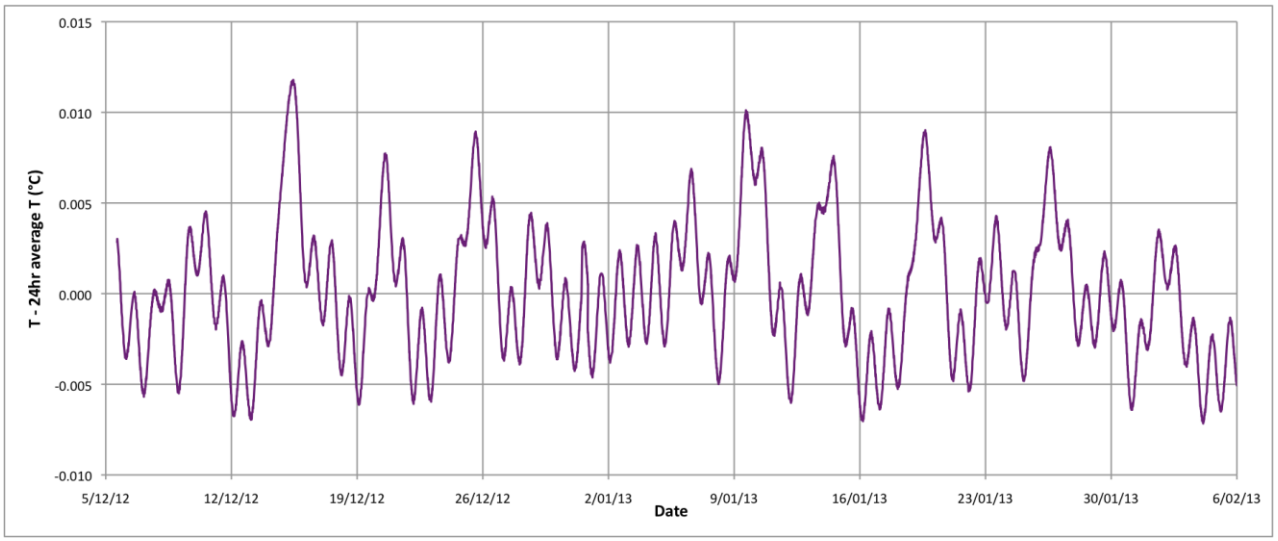

Figure 11: The difference between the instantaneous recorded temperature and the 24-hr moving average temperature at 110 cm depth for the same record as shown on Figure 10. The diurnal temperature cycle is clearly observed with a peak–trough amplitude of about 5 mK, and longer period cycles are also evident.

This paper describes the development of the Heat Needle as an exploration tool, rather than the results of the Carrapateena trial. The Carrapateena trial generated almost 900,000 individual temperature records from the six Heat Needles. As of September 2014, HDR is yet to fully process the data. The interim focus was on refining the hardware design for the next field trial, described below.

4.2 Mexico

In 2013, the Mexican Government approved and funded the formation of the 'Centro Mexicano de Innovación en Energía Geotérmica' (the Mexican Center for Innovation in Geothermal Energy; CEMIE-Geo). Four field trials of the Heat Needle were formally included as Project #23 of the CEMIE-Geo—"Testing probes for measuring shallow heat flow in geothermal zones". The trials commenced in September 2014 with the deployment of six Heat Needles at each of the Los Azufres and Simirao geothermal areas in Mexico. The surveys aim to test the ability of the Heat Needles to map the distribution of surface heat flow at each site. The two surveys will run simultaneously for a six-month period, and then the Heat Needles will be moved to six new sites at each of the Los Humeros and Acoculco geothermal areas for a further six months.

The Mexican trials are testing a new iteration of Heat Needle design. Following the experience of the Carrapateena trial, the new Heat Needles are shorter (1,200 mm), holes are 100% pre-drilled with a single piece premium masonry bit, an additional sensor now collects temperature data at ground level, and the control box sits directly on top of the sensor string. HDR hopes to report on the successful completion of the first two six-month trials during WGC 2015.

5. CONCLUDING REMARKS

The Heat Needle has so far met or exceeded all of the meticulous design criteria to be an exploration tool for geothermal systems, IOCG-U ore bodies, and other subsurface thermal anomalies. HDR's focus has so far been on developing and perfecting the hardware, electronics, calibration process, field procedures and software. So far, data management and manipulation has received less attention, but this will increasingly become HDR's focus as more quality field data are generated. In particular, HDR needs to develop robust mathematical treatments and processes to:

- Derive the vertical thermal diffusivity profile from the diffusion of the surface temperature signal;
- Develope software algorithms to derive 'best-fit' curves of the form described by Equation 7 to heat pulse data;
- Calculate vertical thermal conductivity profiles from diffusivity and volumetric heat capacity;
- Find the best digital low-pass filter to remove the diurnal signal from the thermal gradient data;
- Investigate how to correct the thermal gradient data for lateral variations in vertical thermal diffusivity;
- Demonstrate that the Heat Needle can detect and map lateral variations in vertical conductive heat flow.

6. ACKNOWLEDGEMENTS

Many people and organizations have contributed to the development and testing of the Heat Needle over a number of years. The ongoing project has been carried out as and when funds have been available through sponsorship or when HDR can afford it. Barrick Gold Australia Ltd and Green Rock Energy Ltd has each provided financial sponsorship for Heat Needle development. The University of South Australia has provided both financial and in kind support through transport, storage facilities in Adelaide, and field crew. Oz Minerals Ltd provided substantial 'in kind' support through accommodation and field support at Carrapateena. Chris Pierson of Flawless Fabrications, George Jung of Qwertech Solutions and, more recently, Richard Beale of Featherweight Engineering continue to be major contributors to the design and construction of the hardware, electronics and software that together make up the Heat Needle. Shannon Egan, David Giles, Lawrence Molloy, Jeremy Schulz and Nader Shahin have each donated their time above and beyond the call of duty to calibrate and test the Heat Needles. Most recently, the team at Universidad Michoacana de San Nicolás de Hidalgo in Morelia, Mexico, has provided excellent on-ground support.

REFERENCES

Árnason, K., Eysteinsson, H. and Hersir, G. P.: Joint 1D inversion of TEM and MT data and 3D inversion of MT data in the Hengill area, SW Iceland. *Geothermics*, **39**, (2010), 13–34.

Beardsmore, G.R.: Towards a shallow heat flow probe for mapping thermal anomalies. *Proceedings, 37th Workshop on Geothermal Reservoir Engineering*, Stanford University, Stanford, CA, (2012).

Bullard, E.C.: The flow of heat through the floor of the Atlantic Ocean. *Proceedings, Royal Society of London*, **222**, (1954), 408–429.

Carslaw, H.A. and Jaeger, J.C.: *Conduction of heat in solids, 2nd edition*, Oxford University Press, (1959).

Christoffel, D.A. and Calhaem, I.M.: A geothermal heat flow probe for in situ measurement of both temperature gradient and thermal conductivity, *Journal of Physics E: Scientific Instruments*, **2**, (1969), 457–465.

Coolbaugh, M.F., Sladek, C., Faulds, J.E., Zehner, R.E. and Oppliger, G.L.: Use of rapid temperature measurements at a 2-meter depth to augment deeper temperature gradient drilling. *Proceedings, 32nd Workshop on Geothermal Reservoir Engineering*, Stanford University, Stanford, CA, (2012).

Coolbaugh, M.F., Sladek, C. and Kratt, C.: Compensation for seasonal and surface affects [sic] of shallow (two-meter) temperature measurements. *Transactions, Geothermal Resources Council Annual Meeting*, **34**, (2010), 851–856.

Gerard, R., Langseth, M.G. and Ewing, M.: Thermal gradient measurements in the bottom water and bottom sediment of the Western Atlantic. *Journal of Geophysical Research*, **67**, (1962), 785–803.

Hagermann, A.: Planetary heat flow measurements. *Philosophical Transactions of the Royal Society*, **363**, (2005), 2777–2791.

Houseman, G.A., Cull, J.P., Muir, P.M. and Paterson, H.L.: Geothermal signatures and uranium ore deposits on the Stuart Shelf of South Australia. *Geophysics*, **54(2)**, (1989), 158–170.

Hyndman, R.D., Rodgers, G.C., Bone, M.N., Lister, C.R.B., Wade, U.S. and Barrett, D.L.: Geophysical measurements in the region of the Explorer Ridge of Western Canada. *Canadian Journal of Earth Sciences*, **15**, (1978), 1508–25.

Jeffry, J.A., Chan, T., Cook, N.G.W. and Witherspoon, P.A.: Determination of *in situ* thermal properties of Stripa Granite from temperature measurements in the full-scale heater experiments. Technical Information Report Number 24, *Lawrence Berkeley Laboratory, Earth Sciences Division*, (1979), 34pp.

Kömle, N.I., Hütter, E.S., Macher, W., Kaufmann, E., Kargl, G., Knollenberg, J., Grott, M., Spohn, T., Wawrzaszek, R., Banaszkiewicz, M., Seweryn, K. and Hagermann, A.: *In situ* methods for measuring thermal properties and heat flux on planetary bodies. *Planetary Science Letters*, **59**, (2011), 639–660.

Sladek, C, Coolbaugh, M.F., Penfield, R., Skord, J. and Williamson, L.: The influences of thermal diffusivity and weather on shallow (2-meter) temperature measurements. *Transactions, Geothermal Resources Council Annual Meeting*, **36**, (2012), 793–798.

Steinhart, J.S. and Hart, S.R.: Calibration curves for thermistors. *Deep Sea Research and Oceanographic Abstracts*, **15**, (1968), 497–503.